MODELLING AND SIMULATIONS OF FLAME MITIGATION BY FINE WATER SPRAY

Lipjainen A.L., Snegirev A.Yu.
Saint-Petersburg State Polytechnic University
Email: alex.lipjainen@gmail.com

ABSTRACT

Rapidly growing technology of fire suppression by high-pressure fine water sprays exploits its capability to mitigate gaseous flame faster with smaller water flow rate, yet applying environmentally friendly and toxically safe extinguishing agent. For the optimum use of water in fire suppression, two contradictory requirements should be met: efficient delivery of the dispersed water into the flame zone and rapid droplet evaporation. The most important goals of this work are development of mathematical model of a turbulent evaporating spray, incorporation of the model into the existing in-house Fire3D software, and investigation of the interaction of fine and coarse water sprays with buoyant turbulent diffusion flame. At current moment, major result is that mechanisms of spray-flame interaction are identified, and the drastic differences between the coarse and fine water sprays are demonstrated. For the two distinct cases of flame suppression we demonstrate that the effect of spray refinement depends on the spray-plume momentum ratio.

1. INTRODUCTION

This work is a part of ongoing project of Microsoft Research Corp. and SPbSPU: MicroTEST-FireEx. This project aims to develop the appropriate mathematical model, to incorporate the model into the existing in-house Fire3D software, and to investigate numerically the interaction of fine water spray and buoyant turbulent diffusion flame. As a result, the mechanisms of spray-flame interaction are identified, and the effect of spray characteristics on fire suppression efficiency is determined. In addition to our earlier study [1-2], two cases of flame suppression are considered in this work to demonstrate that the effect of spray refinement depends on the spray-plume momentum ratio.

2. MODEL DESCRIPTION

2.1. Gas phase modeling

The model for the gas phase is the Navier-Stokes equation system for the multicomponent reacting mixture. In this work, URANS simulations are performed by solving Favre-averaged component, momentum and enthalpy transport equations. Modified k-ε model is used to predict mean turbulent fields. Modification of model, closing approaches and discretization of equations were described in [1-2].

2.2. Liquid phase modeling

A Lagrangian approach is applied to model evaporating spray. Given the gas flow characteristics, multiple discrete droplets are tracked along their trajectories, [1-2]. To make computations feasible, the momentum (as well as mass and energy) conservation equation is considered for a group of similar droplets (called as *particle* hereafter).

In addition to mathematical model of evaporating spray at current stage of research we assume that heat flux q_p, received by the particle consists not only of the convective component but also radiative one:

$$q_p = q_{p,conv} + q_{p,rad}\,. \tag{1}$$

The radiative heat flux is

$$q_{p,rad} = -\pi d_p^2 \varepsilon_p \sigma \left(T_p^4 - \frac{G}{4\sigma} \right), \tag{2}$$

where d_p is the droplet diameter, ε_p is the droplet surface emissivity, σ = 5.67·10^{-8} W/(m^2·K^4) is the Stefan-Boltzmann constant, and $G = \int_{\Omega=0}^{4\pi} Id\Omega$ is the incident radiation which is determined when the radiative transfer is simulated.

2.3. Modeling sprinkler spray

Modeling the sprinkler spray implies determination of initial droplet velocity magnitude and direction, diameter and temperature of the discharged liquid when it exhausts through the nozzle being subsequently atomized. The sprinkler is modeled here as a point source of droplets having velocity vectors uniformly distributed inside the cone of angle φ. The nozzle is located at the vertical flame axis and the spray axis is directed downward. Mean droplet velocity is taken equal to velocity of liquid discharging through the nozzle:

$$V_{p,0} = \varsigma \sqrt{\frac{2\Delta P_S}{\rho_p}}, \ \varsigma < 1, \tag{3}$$

where ΔP_S is the excess pressure in the water supply piping. Gaussian distribution is assumed for individual particle velocities, with the mean value of $V_{p,0}$ and the root mean square deviation of $0.1 V_{p,0}$.

In this work sprinkler has the wide cone angle of φ = 120º, nozzle diameter of D_0 = 3.97 mm to replicate data [3]. Water flow rates were varied from 2 to 15 l/min. The value of K-factor (proportionality coefficient between the flow rate and excess pressure in the piping) of the nozzle K = 0.76 l/(min·kPa$^{1/2}$) given in [3] is used to estimate the discharge coefficient ς: $\varsigma = K \big/ A\sqrt{2/\rho_p}$ = 0.72, where $A = \pi D_0^2/4$ = 1.24·10^{-5} m^2 is the nozzle cross-section area. Flow rate of 11.17 l/min corresponds to the liquid discharge velocity (and therefore mean initial droplet velocity) of $V_{p,0}$ = 15 m/s and the excess pressure of $\Delta P_S = \left(V_{p,0} A/K\right)^2$ = 216 kPa. The increase of the excess pressure ΔP_S results in finer droplets produced by the nozzle :

$$\frac{d}{d_{ref}} \propto \left(\frac{\Delta P_{S,ref}}{\Delta P_S} \right)^{0.3}. \tag{4}$$

Initial median droplet diameter of d_{v50} = 0.721 mm is reported in [3] for the excess pressure of ΔP_S = 137.9 kPa. Using correlation for the above estimated value of ΔP_S = 216 kPa the median droplet diameter d_{v50} = 0.630 mm is obtained. The spray having the initial median droplet diameter of 0.630 mm is called below as the *coarse* one. In view of the aim of this work to investigate the effects of fine water atomization, we also consider the spray with the initial median droplet diameter of 0.080 mm (*fine* spray). To identify the effects of initial spray dispersion, we keep $V_{p,0}$ = 15 m/s in all the simulations performed in this work.

3. RESULTS AND DISCUSSION

In the simulations, the experimental conditions were replicated where the water spray suppressed buoyant turbulent diffusion flames, either at small [3] or large [4] scales. In the first case (small scale), the flame was produced by the methane-fuelled burner with the exit surface (18 cm diameter) located at the floor level. In accordance to the burner design [3], fuel velocity was assumed to be uniformly distributed over the exit surface and directed normally to the surface. Fuel flow rate corresponds to the flame calorific power of $\dot{Q}$ = 15 kW. In the second case (large scale), a 2 m diameter pool fire is considered with calorific power of $\dot{Q}$ = 2.46 MW.

In both cases the simulation methodology includes two stages. The first one is the transient simulation of the gas flame in the open space above the burner until steady state (without spray). The results are then used as initial conditions for the second stage when transient spray discharge, spread, evaporation and interaction with the flame is considered. The simulations have been performed in 3×3×3 m computational domain. Both the burner and the sprinkler nozzle are located at the central axis. In the computations, 40^3 to 64^3 grids are used, with the refinement near the flame axis.

3.1. The effect of spray dispersion on its dynamics and structure

It was found that the decrease in the initial droplet diameter drastically changes the spray dynamics and the mode of its interaction with flame (Fig. 1). First of all, the relaxation times are reduced: smaller droplets rapidly relax to both dynamic and thermal equilibrium with carrying phase thereby getting driven by the gas flow. The estimates show that 630 μ initial diameter (coarse spray) and 15 m/s initial velocity droplets retain their momentum up to a distance of 2 m while their 80 μ counterparts lose its momentum at a distance of an order of magnitude less.

Secondly, the carrying gas flow itself is formed by the spray and is directly affected by the spray momentum. The simulations have shown that in the vicinity of spray the adjacent cocurrent flow forms that entrains the air towards the spray axis. Such an entraining flow has virtually no effect on the large droplets, and as a result the shape of the coarse spray is determined by the initial spray spread angle and therefore by the nozzle geometry. Alternatively, the above mentioned entraining flow concentrates and narrows the spray by driving small particles towards the spray axis. That causes fine water spray to be narrow-shaped, and its axial velocity to be greater than that at the coarser spray provided the total spray momentum is the same. Thus, the shape of the *coarse* spray is determined by the initial spray spreading angle, and, alternatively, *fine* water spray is of much smaller diameter which is controlled by the toroidal large-scale vortex surrounding the spray and creating the entraining gas flow.

Finally, due to the greater droplet surface area per unit flow rate, droplet evaporation rate and vapor concentration increase and the droplet lifetime decreases.

3.2. Why finer spray suppresses flame more rapidly?

The simulation results indicate that for the same flow rates and droplet velocity distributions (velocity magnitude and cone shape), finer spray suppresses flame more rapidly than the coarse one. This is illustrated by Fig. 2 *a*, where the predicted maximum value of the mean flame temperature is shown as a function of time.

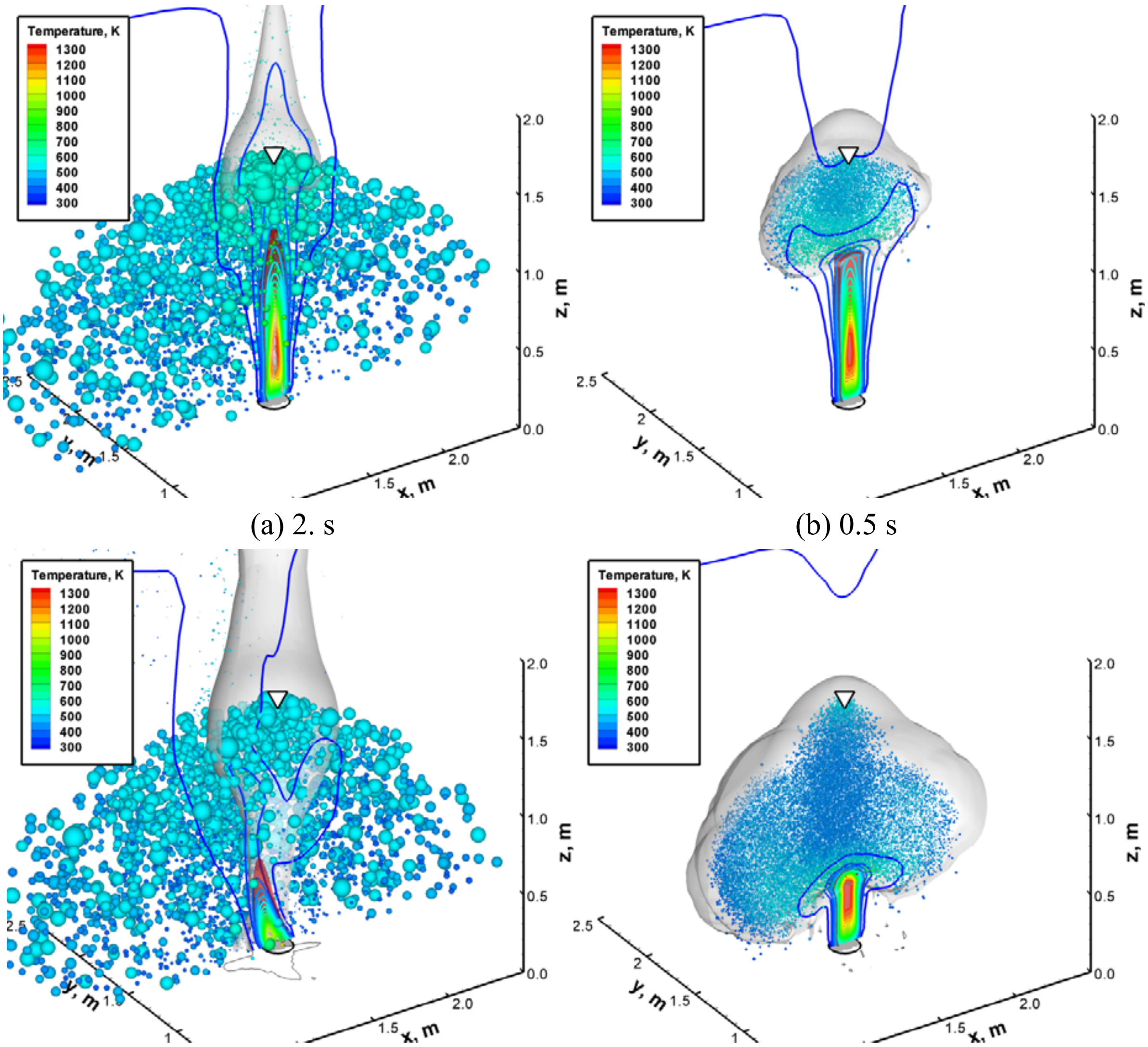

(a) 2. s (b) 0.5 s

(c) 17 s (d) 1.3 s

Figure 1. Flame suppression by symmetric water sprays (water flow rate is 7.57 l/min): *a*, *c* – coarse spray, initial median droplet diameter 0.630 mm (2.0, 17 s after nozzle activation); *b*, *d* – fine spray, initial median droplet diameter 0.080 mm (0.5, 1.3 s after nozzle activation). Transparent surface shows 0.2% volume fraction of vaporized water

It can be seen that at a flow rate of 7.57 l/min the coarse spray does not significantly affect the flame during the observation period, while the fine spray extinguishes the flame within few seconds after the nozzle activation.

One of the reasons for such a remarkable difference is shown in Fig. 2 *b*, which demonstrates the rate of vapor generation upon spray evaporation. The fine spray produces the amount of vapor which is by more than an order of magnitude greater than that produced by the coarse spray. It has also been found that in the coarse spray evaporated fraction (portion of the evaporated mass per unit time in the total water flow rate) is about 1% regardless of the flow rate. It means that vast majority of water is transported to the solid walls rather than evaporated to affect the gas flame. Proportionality of the evaporation rate to the nozzle flow rate (Fig. 3 *a*) also indicates that the evaporation occurs in a low vapor concentration (which is confirmed by the simulation results). Alternatively, in the fine spray the evaporated fraction varies from 15 to 30%, and the increase of the flow rate causes observable decrease in the evaporated fraction although absolute value of the evaporation rate increases (Fig. 3 *b*). The latter is indicative of the high vapor concentration in the gas phase surrounding evaporating droplets and reducing evaporation rate.

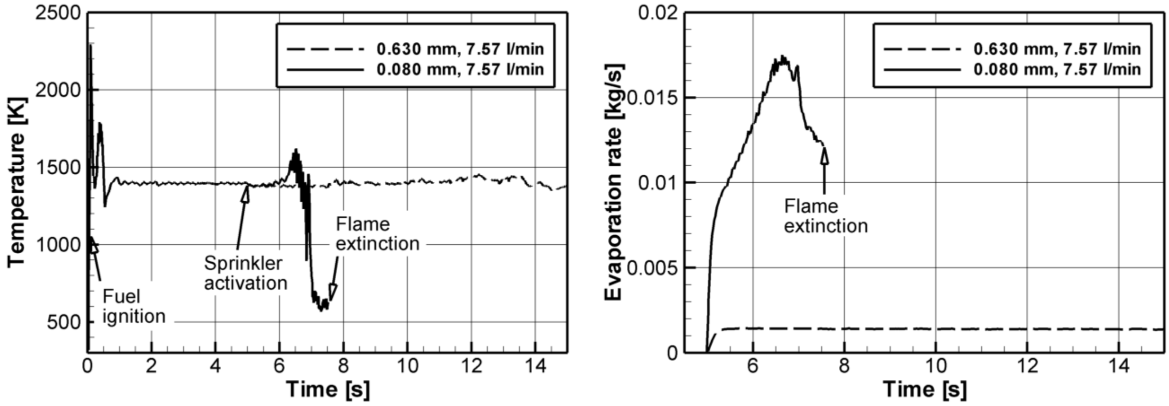

(a) (b)

Figure 2. The effect of initial spray dispersion on transient spray-flame interaction: *a* – mean flame temperature (maximum value); *b* – spray evaporation rate

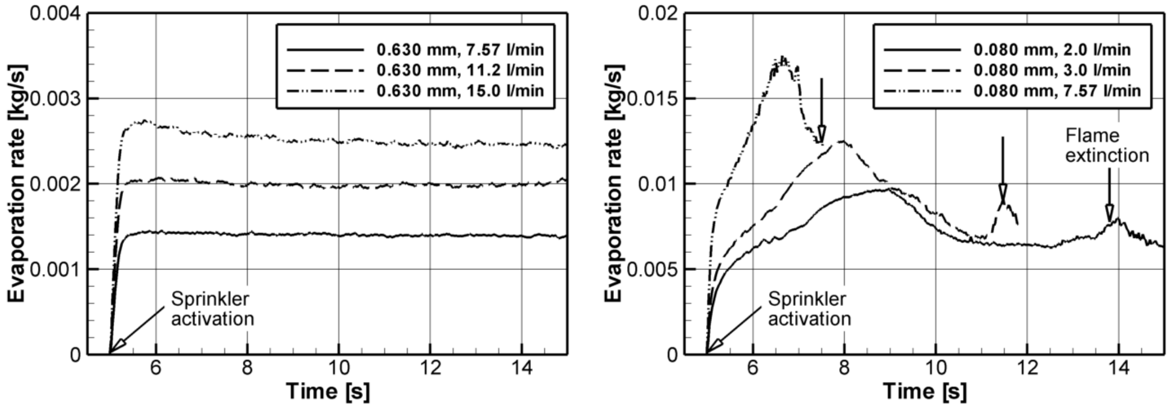

(a) (b)

Figure 3. Transient spray evaporation rate: *a* – coarse spray (initial median droplet diameter 0.630 mm); *b* – fine spray (initial median droplet diameter 0. 080 mm)

Another reason of the dramatic difference in the intensity of flame mitigation by the two sprays considered is in different mechanisms of spray-flame interactions. Firstly, more rapid spray evaporation results in much higher velocity of the gas flow carrying droplets (note that total flow momentum is the same). Thus, large droplets in a coarse spray keep its momentum until they reach the walls while droplet momentum in a fine spray is nearly completely transferred to thus accelerated gas flow. Hence, the faster flame mitigation by the fine sprays.

It is also important that the large droplets easily penetrate into the flaming region where its evaporation rate increases thereby creating local maximum of vapor concentration *inside* the flame. Alternatively, fine droplets cannot penetrate inside the flame being deflected by the gas flow. Instead, they form the vapor cloud that surrounds the flame from the *outside*. This explains why fine water spray (mist) is most suitable as a total flooding agent in closed compartments where gas flame mitigation is a primary target of fire suppression.

The above trends are clearly seen in Fig. 1, which compares transient spray flame interactions for the coarse and fine sprays at the same water flow rates of 7.57 l/min. It can be observed that the symmetric coarse spray destabilizes flame but does not extinguish it for a rather long time of exposure, while the symmetric fine spray suppresses the flame in a few seconds.

3.3. Spray dispersion may not be advantageous

The above scenario corresponding to Schwille and Lueptow experimental conditions [3] can be characterized as the spray cone that is much wider than the flame base. Furthermore, spray momentum (if concentrated around the fuel source) is apparently higher than that of the rising flame driven flow.

We are going to illustrate here that these conditions are not universal for fire suppression, and, accordingly, refining spray dispersion may not guarantee more efficient flame mitigation. To demonstrate this, we consider another scenario of fire suppression taken from the ongoing experimental programme by Sandia Laboratories. Data reported in [4] have been obtained in the Fire Laboratory for Accreditation of Models and Experiments (FLAME) for 2 m diameter liquid pool fire (2.46 MW) attacked by the spray with 30º cone angle, originated from the sprinkler located 5 m height above the pool surface. In the simulations performed in this work, droplet size distributions with median diameters d_{v50} from 0.250 to 0.750 mm and water flow rates from 106 to 212 l/min are considered. Prior to the nozzle activation, a steady flame has been simulated.

This case is indeed distinctive from the Schwille and Lueptow experiment [4] at least because of the fact that the spray projection just covers the pool. Another difference stems from the exceeding momentum of rising flow.

In the simulation results shown in Fig. 4, the upper row of figures shows the droplets colored in accordance with their temperature (300 K (blue) – 373 K (red)) and sized by their predicted diameter, while the lower row of figures shows gas velocity field in the flame axial cross section (arrows colored by mean temperature, 300 K (blue) – 1300 K (red)). All the figures include iso-surfaces corresponding to 1 MW/m^3 heat release rate (red) and 0.8% vapor mole fraction (gray).

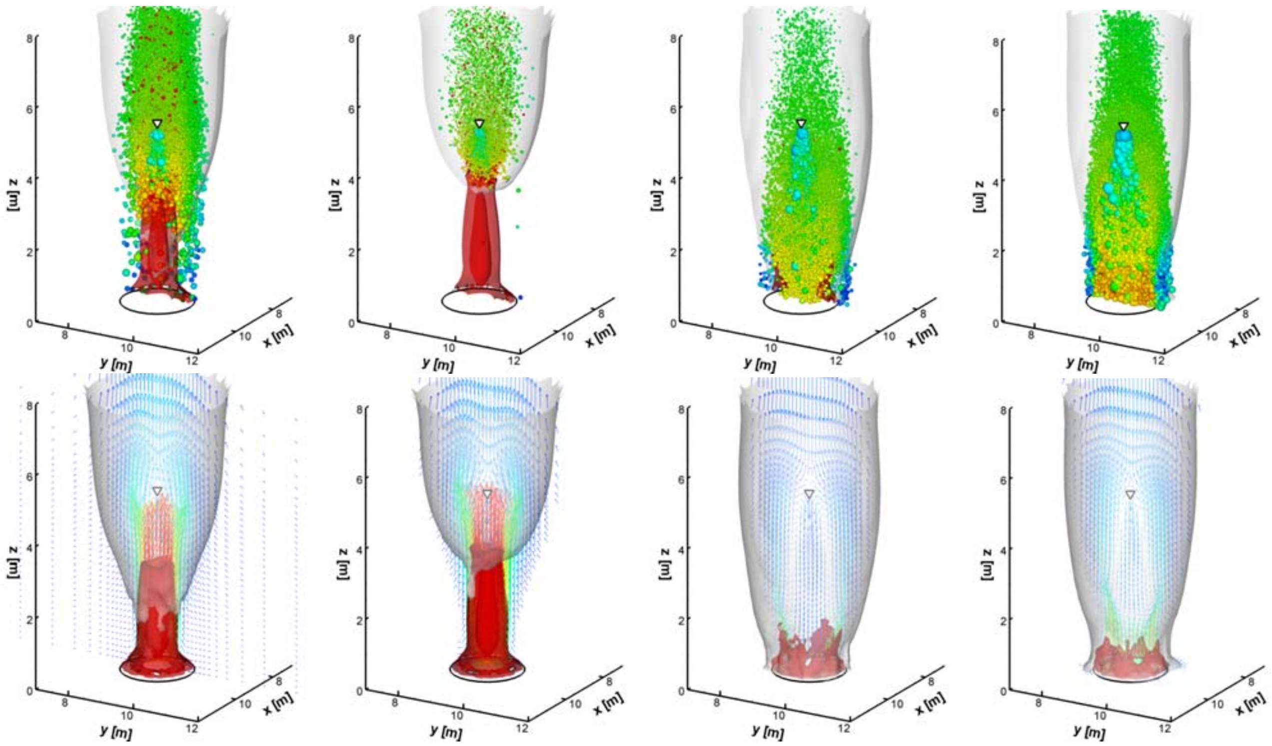

(a) (b) (c) (d)

Figure 4. Water mist flame suppression of 2.46 MW, 3 s after spray initiation:
a - water flow rate 106 l/min, initial droplet velocity V_0 = 15 m/s, initial d_{v50} = 0.500 mm;
b - water flow rate 106 l/min, initial droplet velocity V_0 = 15 m/s, initial d_{v50} = 0.250 mm;
c - water flow rate 212 l/min, initial droplet velocity V_0 = 15 m/s, initial d_{v50} = 0.500 mm;
d - water flow rate 212 l/min, initial droplet velocity V_0 = 15 m/s, initial d_{v50} = 0.750 mm

The following conclusions have been derived from the simulation analysis.

Given the droplet size distribution, spray momentum might be insufficient to suppress flame. In this case, larger droplets still penetrate the flame zone and evaporate there but cannot considerably affect the flame. Major part of the spray is deflected upwards by the flame-driven rising flow (Fig. 4 *a*). Rising flow is a reason why in contrast to the above predictions for the 15 kW flame, finer spray (Fig. 4 *b*, 106 l/min, V_0 = 15 m/s, d_{v50} = 0.250 mm) does not perform better. In this case decrease in initial droplet diameter was found to be useless.

At sufficient momentum (e.g. that shown in Fig. 4 *c*, 212 l/min, V_0 = 15 m/s, d_{v50} = 0.500 mm) spray approaches the pool surface thereby extinguishing the fire despite the relatively coarse droplet dispersion. Furthermore, in this case coarser spray (Fig. 4 *d*, 212 l/min, V_0 = 15 m/s, d_{v50} = 0.750 mm) approaches pool surface more rapidly.

As a result, fine spray momentum is insufficient to get over the momentum of fire-driven flow, and in this case spray refinement is not an advantageous solution for faster fire extinguishment. Clearly, more work is required to identify quantitative criteria that can generalize these conclusions for a wider range of practically important scenarios.

4. CONCLUSIONS

The model is presented of the evaporating spray that affects the buoyant turbulent diffusion flame. Better understanding of physics and ability to accurately predict the spray-flame interaction is sought, with the ultimate aim to contribute into design of the efficient and environmentally friendly halon-free fire suppression methodology.

The model is incorporated into the existing CFD software Fire3D and applied to predict the effect of the initial droplet size distribution on the spray-flame interaction. Simulation results have shown that the fire scenario is possible, when fine water spray causes faster flame extinguishment with smaller water flow rate.

The above advantages of fire suppression technology by high-pressure fine water sprays are therefore expected to be exploited at an increasing number of applications where the minimizing water flow rate is of vital importance.

REFERENCES

1. Lipjainen A.L. Simulation of the Fire Extinguishment Process by Fine Water Spray // JASS 2008, http://www14.informatik.tu-muenchen.de/konferenzen/Jass08/courses/5/
2. A.Yu. Snegirev, A.L. Lipjainen, Modeling and simulations of fine water spray in buoyant turbulent diffusion flame // Heat Transfer Research. Vol. 39, issue 2, 2008. - p. 133-149.
3. Schwille J.A., Lueptow R.M. The reaction of a fire plume to a droplet spray // Fire Safety Journal, Vol. 41, 2006, 390–398
4. Blanchat T.K., Nichols R.T., Figueroa V.G. Benchmark Enclosure Fire Suppression Experiments – Phase 1 Test Report // Sandia Report SAND2007-3220, Sandia National Labs, 2007.